Computer Assisted Mechanics and Engineering Sciences, 13: 537–546, 2006.

Thin layer shear and second order homogenization method

Łukasz Kaczmarczyk
Cracow University of Technology, Institute for Computational Civil Engineering
ul. Warszawska 24, 31-155 Kraków, Poland

(Received in the final form October31, 2006)

This paper deals with the second-order computational homogenisation of a heterogeneous material undergoing small displacements. Typically, in this approach a representative volume element (RVE) of nonlinear heterogeneous material is defined. An a priori given discretised microstructure is considered, without focusing on detailed specific discretisation techniques. The key contribution of this paper is the formulation of equations coupling micro- and macro-variables and the definition of generalized boundary conditions for the microstructure. The coupling between macroscopic and microscopic levels is based on Hill's averaging theorem. We focus on deformation-driven microstructures where overall macroscopic deformation is controlled. In the end a numerical example of a thin layer shear is presented.

1. Introduction

A wide range of materials produced by industry as well as natural materials are heterogeneous at a certain scale of observation. The macroscopic (equivalent) properties of a heterogeneous material should describe the essence of microstructural response. It must be independent of its macrostructural loads or geometry. The micro-to-macro transitions have to be consistent with the basic principles of continuum mechanics, i.e. they are subjected to principles of conservation of mass, momentum, energy, and to the Clausius–Duhem inequality.

A comprehensive review of overall properties of heterogeneous materials is provided in [9]. Equivalent material properties are obtained as a result of analytical or semi-analytical solution. In recent years a promising alternative approach has been developed, i.e. computational homogenisation [5]. This micro-macro modelling procedure does not lead to closed-form constitutive relations, but computes on line the strain-stress relationship at a selected point with attributed detailed microstructure assigned to that point. This approach does not require any constitutive assumption on the macro level and enables the incorporation of nonlinear geometric and material equations [2, 5]. The computational homogenisation analysis is possible for any discretisation technique in space and time.

In the paper a well-known framework of linking material properties at two levels of material description is presented. The materials heterogeneous on one level (microscale), while the material is considered homogeneous at macroscale level of observation. There are a number of strategies which are used in multiscale analysis. In this paper we discuss a numerical approach, i.e. computational homogenisation Fig. 1.

After [3], multiscale models are constructed using three main ingredients Fig. 2:

1. modelling of mechanical behaviour at microscale (representative volume element RVE),
2. localisation rule which determines the local solution inside RVE for given macroscopic deformation measures,
3. homogenisation rule giving the macroscopic stress measures, knowing the micromechanical stress state.

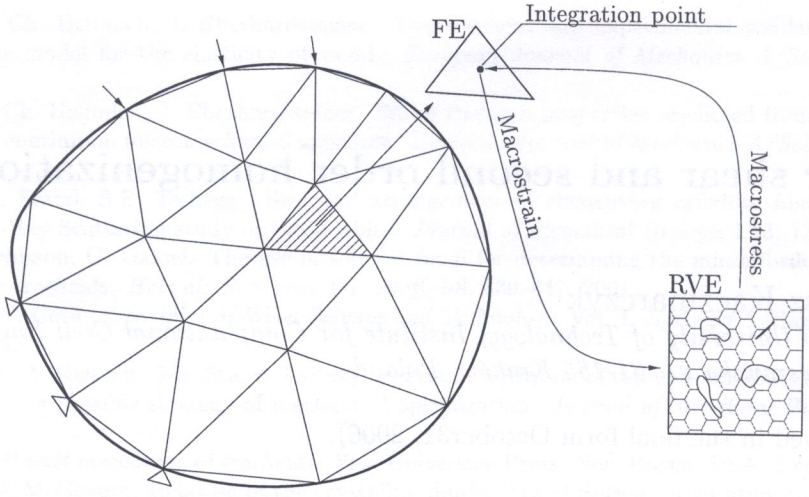

Fig. 1. Computational homogenisation

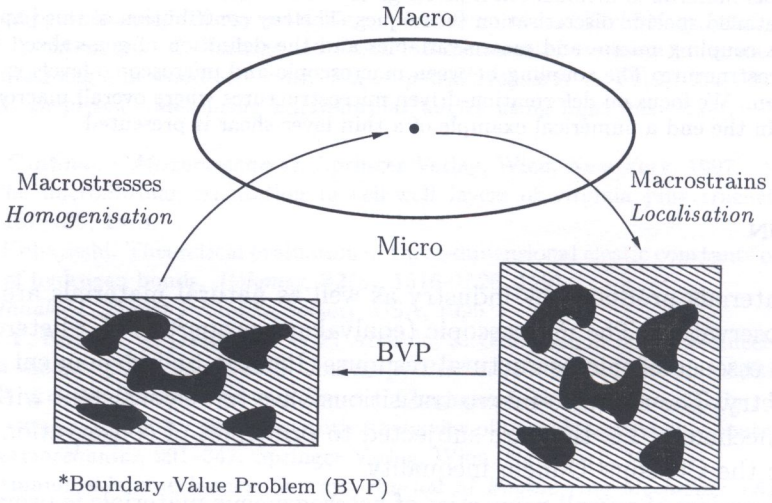

Fig. 2. Computing nonhomogeneous material response

In Section 2 the boundary equations as well as the macrostrain and macrostress expressed in terms of displacements and traction forces on the boundary of RVE are given. In Section 3 after finite element discretisation and deformation driven microstructures, the overall stresses and tangent moduli are defined only in terms of discrete forces and stiffness properties of RVE. To enforce boundary conditions and to compute stresses and tangent moduli the projection matrices are used. In Section 4 a numerical solution of a thin layer shear for a porous material is presented. In the end conclusions are presented.

2. Macro to micro and micro to macro transitions

The paper concentrates on some issues of a fully coupled second order homogenisation scheme. Attention is focused on micro-macro transitions of the discretised microstructure. A new approach is proposed which can handle any type of boundary conditions (i.e. displacement, periodic and static boundary conditions). The boundary conditions enforce the deformation of representative volume element (RVE) according to a given gradient and second gradient of displacements in average sense. We note that the method is used to couple two different continua: classical one at the microscale,

and Mindlin's continuum [8] at the macroscale. After expansion of the displacement vector at the geometric centre of RVE and truncation after the second-order term we obtain

$$\mathbf{u}(\mathbf{X},\mathbf{x}) = \mathbf{u}^0(\mathbf{X}) + \mathbf{x}\cdot\overline{\boldsymbol{\varepsilon}}(\mathbf{X}) + \frac{1}{2}\mathbf{x}\otimes\mathbf{x} : \overline{\boldsymbol{\eta}}(\mathbf{X}) + \mathbf{r}(\mathbf{X},\mathbf{x}), \tag{1}$$

where $\overline{\boldsymbol{\varepsilon}} = \mathrm{sym}[\mathrm{grad}[\mathbf{u}]]$ is the macrostrain tensor, $\overline{\boldsymbol{\eta}} = \mathrm{grad}[\mathrm{grad}[\mathbf{u}]]$ is the second-order macroscopic strain tensor, $\mathbf{r}$ is the microfluctuation of displacement added to fulfill the equilibrium equation in RVE.

The boundary conditions can be written in an integral form as

$$\int_\Gamma \delta\mathbf{t}\cdot\mathbf{r}\,\mathrm{d}\Gamma = 0, \qquad \int_\Gamma \mathbf{n}\otimes\mathbf{r}\,\mathrm{d}\Gamma = \mathbf{0}, \qquad \int_\Gamma \mathbf{n}\otimes\mathbf{x}\otimes\mathbf{r}\,\mathrm{d}\Gamma = \mathbf{0}, \tag{2}$$

where $\mathbf{n}$ is the normal vector field and $\delta\mathbf{t}$ is a statically admissible variation of tractions on the boundary. If the first integral satisfies Hill–Mandel theorem, the second and third integrals enforce the deformation of RVE according to a given macrostrain tensor and given gradient of macrodeformation tensor in an average sense, correspondingly. For further FE discretisation, the boundary conditions can be expressed in terms of microscopic displacement tensor and macrostrains,

$$\int_\Gamma \delta\mathbf{t}\cdot\left(\mathbf{u} - \mathbf{x}\cdot\overline{\boldsymbol{\varepsilon}} - \frac{1}{2}\mathbf{x}\otimes\mathbf{x} : \overline{\boldsymbol{\eta}}\right)\mathrm{d}\Gamma = 0, \tag{3}$$

$$\int_\Gamma \mathbf{n}\otimes\left(\delta\mathbf{u} - \mathbf{x}\cdot\overline{\boldsymbol{\varepsilon}} - \frac{1}{2}\mathbf{x}\otimes\mathbf{x} : \overline{\boldsymbol{\eta}}\right)\mathrm{d}\Gamma = \mathbf{0}, \tag{4}$$

$$\int_\Gamma \mathbf{n}\otimes\mathbf{x}\otimes\left(\delta\mathbf{u} - \mathbf{x}\cdot\overline{\boldsymbol{\varepsilon}} - \frac{1}{2}\mathbf{x}\otimes\mathbf{x} : \overline{\boldsymbol{\eta}}\right)\mathrm{d}\Gamma = \mathbf{0}. \tag{5}$$

To make the model complete, the macroscopic strain and stress measures in terms of microquantities are given. For a statistically homogeneous body macroscopic quantities can be defined as averaged microquantities over volume RVE [9], for simplicity, for the geometrically linear problem we have

$$\overline{\boldsymbol{\varepsilon}} = \frac{1}{V}\int_\Gamma \mathbf{n}\otimes\mathbf{u}\,\mathrm{d}\Gamma, \tag{6}$$

$$\overline{\boldsymbol{\sigma}} = \frac{1}{V}\int_\Gamma \mathbf{x}\otimes\mathbf{t}\,\mathrm{d}\Gamma, \tag{7}$$

$$\frac{1}{2}\int_V (\mathbf{x}\otimes\mathbf{x}\otimes\mathbf{1} + \mathbf{x}\otimes\mathbf{1}\otimes\mathbf{x} + \mathbf{1}\otimes\mathbf{x}\otimes\mathbf{x})\,\mathrm{d}V : \overline{\boldsymbol{\eta}} = \int_\Gamma \mathbf{n}\otimes\mathbf{x}\otimes\mathbf{u}\,\mathrm{d}\Gamma, \tag{8}$$

$$\overline{\boldsymbol{\tau}} = \frac{1}{2V}\int_\Gamma \mathbf{x}\otimes\mathbf{x}\otimes\mathbf{t}\,\mathrm{d}\Gamma, \tag{9}$$

where $\overline{\boldsymbol{\sigma}}$ is second-order macrostress tensor work-conjugate to $\overline{\boldsymbol{\varepsilon}}$, $\overline{\boldsymbol{\tau}}$ is third-order macrostress tensor work-conjugate to $\overline{\boldsymbol{\eta}}$. It can be noted that macro quantities are given exclusively by displacements and traction forces on the boundary of RVE. According to Hill–Mandel theorem it can be shown that for the given equations the work of macrostrains on macrostresses is equal to the work of microstrains on microstresses in the RVE attached to a macroscopic point.

3. Finite element discretisation and enforcing boundary conditions for RVE

The application of boundary conditions and other constraints to the stiffness matrix and load vector is an integral part of the finite element code. This process can pose difficulties when certain combinations of boundary conditions for RVE occur. A general approach to the problem of enforcing constraints for any finite element code is shown in [1].

After FE discretisation of RVE the vector of the nodal displacements $\mathbf{u}$ is defined as a solution of the constrained quadratic programming problem:

$$\begin{aligned} &\min_{\mathbf{u}} \quad \mathcal{Q} = \tfrac{1}{2}\mathbf{u}^{\mathrm{T}}\mathbf{K}\mathbf{u} - \mathbf{u}^{\mathrm{T}}\mathbf{F}, \\ &\text{subject to} \quad \mathbf{C}\mathbf{u} - \mathbf{g} = \mathbf{0}, \end{aligned} \tag{10}$$

where $\mathbf{K}$ is the stiffness matrix, $\mathbf{F}$ is the load vector, $\mathbf{C}$ is constraint matrix and $\mathbf{g}$ is the displacement constraint vector. The common solution method is to introduce Lagrange multipliers $\boldsymbol{\lambda}$,

$$\mathcal{L} = \frac{1}{2}\mathbf{u}^{\mathrm{T}}\mathbf{K}\mathbf{u} - \mathbf{u}^{\mathrm{T}}\mathbf{F} + \boldsymbol{\lambda}^{\mathrm{T}}(\mathbf{C}\mathbf{u} - \mathbf{g}). \tag{11}$$

The Euler conditions for the stationary point of the Lagrangian are found to be

$$\mathbf{K}\mathbf{u} + \mathbf{C}^{\mathrm{T}}\boldsymbol{\lambda} = \mathbf{F}, \qquad \mathbf{C}\mathbf{u} = \mathbf{g}. \tag{12}$$

However, this approach increases the number of unknowns and the character of the matrix is altered (to an indefinite saddle point problem). The numerical solution of such a problem is inefficient, so it is not adequate for solving computationally complex multiscale problems, where for each Gauss integration point the solution of the constrained quadratic problem has to be found.

In papers [6, 7] the solution for micro-to-macro transition of discretised microstructure by the computation of condensed matrices, associated with the boundary of RVE, can be found. In this paper an alternative approach to solving such problems in case of second-order homogenisation is presented. On the assumption that the problem is well-posed, the following matrices are well defined,

$$\mathbf{Q} = \mathbf{I} - \mathbf{R}\mathbf{C}, \tag{13}$$

$$\mathbf{R} = \mathbf{C}^{\mathrm{T}}(\mathbf{C}\mathbf{C}^{\mathrm{T}})^{-1}. \tag{14}$$

where $\mathbf{R}$ is the auxiliary matrix and $\mathbf{Q}$ is the projection matrix. If matrix $\widetilde{\mathbf{K}}$ and the right-hand vector $\widetilde{\mathbf{F}}$ are defined by expressions

$$\widetilde{\mathbf{K}} = \mathbf{C}^{\mathrm{T}}\mathbf{C} + \mathbf{Q}^{\mathrm{T}}\mathbf{K}\mathbf{Q}, \tag{15}$$

$$\widetilde{\mathbf{F}} = \mathbf{C}^{\mathrm{T}}\mathbf{g} + \mathbf{Q}^{\mathrm{T}}(\mathbf{F} - \mathbf{K}\mathbf{R}\mathbf{g}), \tag{16}$$

there exists a unique solution $\mathbf{u}$ of the problem (10),

$$\widetilde{\mathbf{K}}\mathbf{u} = \widetilde{\mathbf{F}}, \tag{17}$$

and the Lagrange multipliers are given by

$$\boldsymbol{\lambda} = \mathbf{R}^{\mathrm{T}}(\mathbf{F} - \mathbf{K}\mathbf{u}). \tag{18}$$

Matrix $\widetilde{\mathbf{K}}$ involves the computation of global stiffness matrix $\mathbf{K}$. However, in practical computations there is no need to perform global operations on matrices, or to assemble global matrix $\mathbf{K}$. Enforcing constraints can be performed by subassembly procedure element by element [1].

This approach enables one to apply any boundary condition, e.g. displacement, periodic or traction boundary conditions on the boundary of RVE. This method can also be easily applied to any shape of RVE.

3.1. Matrix form of boundary conditions

After FE discretisation of RVE the boundary conditions (3)–(5) can be written in a matrix form as

$$\mathbf{Cu} = \mathbf{D}\overline{\boldsymbol{\varepsilon}} + \mathbf{E}\overline{\boldsymbol{\eta}} = \mathbf{g}. \tag{19}$$

Matrix $\mathbf{C}$ is given by

$$\mathbf{C} = \int_{\Gamma} \mathbf{H}\mathbf{N}^{\mathrm{T}}\mathbf{N}\,\mathrm{d}\Gamma, \tag{20}$$

where matrices $\mathbf{D}$ and $\mathbf{E}$ are in the form

$$\mathbf{D} = \int_{\Gamma} \mathbf{H}\mathbf{N}^{\mathrm{T}}\mathbf{X}\,\mathrm{d}\Gamma, \tag{21}$$

$$\mathbf{E} = \int_{\Gamma} \mathbf{H}\mathbf{N}^{\mathrm{T}}\mathbf{Z}\,\mathrm{d}\Gamma, \tag{22}$$

$\mathbf{N}$ is the matrix of shape functions, and matrices $\mathbf{X}$ and $\mathbf{Z}$ are defined by

$$\mathbf{X} = \frac{1}{2}\begin{bmatrix} 2x & 0 & y \\ 0 & 2y & x \end{bmatrix}, \tag{23}$$

$$\mathbf{Z} = \frac{1}{4}\begin{bmatrix} 2x^2 & 0 & 2y^2 & 0 & xy & 0 \\ 0 & 2y^2 & 0 & 2x^2 & 0 & xy \end{bmatrix}. \tag{24}$$

In each row of matrix $\mathbf{H}$ there are nodal values of admissible distribution of traction forces on the boundary of RVE. For example, in case of the first-order homogenisation and periodic boundary conditions all antiperiodic and self-equilibrated boundary conditions are admissible. Matrix $\mathbf{H}$ contains nodal values of all linearly independent antiperiodic self-equilibrated distributions of traction on the boundary of RVE.

3.2. Computation stress and higher order stress

If the equilibrium equation is fulfilled, the work of displacements on tractions is equal to the work of generalized displacements on Lagrange multipliers,

$$\mathbf{u}^{\mathrm{T}}\mathbf{t} = (\mathbf{D}\overline{\boldsymbol{\varepsilon}} + \mathbf{E}\overline{\boldsymbol{\eta}})^{\mathrm{T}}\boldsymbol{\lambda}. \tag{25}$$

Following the solution of boundary value problem according to Hill–Mandel theorem, the first-order macrostress vector is given in terms of the Lagrange multiplier vector and matrix $\mathbf{D}$,

$$\overline{\boldsymbol{\sigma}} = \frac{1}{V}\mathbf{D}^{\mathrm{T}}\boldsymbol{\lambda}, \tag{26}$$

and the second-order macrostress vector is given in terms of the Lagrange multiplier vector and matrix $\mathbf{E}$,

$$\overline{\boldsymbol{\tau}} = \frac{1}{V}\mathbf{E}^{\mathrm{T}}\boldsymbol{\lambda}. \tag{27}$$

3.3. Computation of tangent matrices

Closed-form stress-strain relation is unknown at all the stages of the computational homogenisation approach. For the finite element method at the macro level only the material tangent stiffness matrices and stress vectors or increments of strain vectors have to be determined at each Gauss integration point. The linearized relation between strain increments and stress increments for the second-order continuum are given by

$$\Delta\overline{\boldsymbol{\sigma}} = \overline{\mathbf{C}}^1\Delta\overline{\boldsymbol{\varepsilon}} + \overline{\mathbf{C}}^2\Delta\overline{\boldsymbol{\eta}}, \tag{28}$$

$$\Delta\overline{\boldsymbol{\tau}} = \overline{\mathbf{C}}^3\Delta\overline{\boldsymbol{\varepsilon}} + \overline{\mathbf{C}}^4\Delta\overline{\boldsymbol{\eta}}. \tag{29}$$

To compute tangent stiffness matrices, $(3+6+3+6)$ linear equations at equilibrium for each RVE have to be solved. For example, material tangent stiffness matrix $\overline{\mathbf{C}}^1$ is computed as

$$\overline{\mathbf{C}}^1 = [\,\delta\overline{\boldsymbol{\sigma}}^1\,,\,\delta\overline{\boldsymbol{\sigma}}^2\,,\,\delta\overline{\boldsymbol{\sigma}}^3\,], \tag{30}$$

where columns $\delta\overline{\boldsymbol{\sigma}}^i$, $i = 1,2,3$, are computed for given increments of the strain vectors,

$$\begin{aligned}
&\delta\overline{\boldsymbol{\sigma}}^1: \quad \text{for} \quad \delta\overline{\boldsymbol{\varepsilon}} = [1\,0\,0]^{\mathrm{T}}, \quad \delta\overline{\boldsymbol{\eta}} = [0\,0\,0\,0\,0\,0]^{\mathrm{T}},\\
&\delta\overline{\boldsymbol{\sigma}}^2: \quad \text{for} \quad \delta\overline{\boldsymbol{\varepsilon}} = [0\,1\,0]^{\mathrm{T}}, \quad \delta\overline{\boldsymbol{\eta}} = [0\,0\,0\,0\,0\,0]^{\mathrm{T}},\\
&\delta\overline{\boldsymbol{\sigma}}^3: \quad \text{for} \quad \delta\overline{\boldsymbol{\varepsilon}} = [0\,0\,1]^{\mathrm{T}}, \quad \delta\overline{\boldsymbol{\eta}} = [0\,0\,0\,0\,0\,0]^{\mathrm{T}}.
\end{aligned} \tag{31}$$

Material tangent stiffness matrix $\overline{\mathbf{C}}^2$ is computed as

$$\overline{\mathbf{C}}^2 = [\,\delta\overline{\boldsymbol{\sigma}}^1\,,\,\delta\overline{\boldsymbol{\sigma}}^2\,,\,\delta\overline{\boldsymbol{\sigma}}^3\,,\,\delta\overline{\boldsymbol{\sigma}}^4\,,\,\delta\overline{\boldsymbol{\sigma}}^5\,,\,\delta\overline{\boldsymbol{\sigma}}^6\,], \tag{32}$$

where columns $\delta\overline{\boldsymbol{\sigma}}^i$, $i = 1,\ldots,6$, are computed for given increments of the higher order strain vector,

$$\begin{aligned}
&\delta\overline{\boldsymbol{\sigma}}^1: \quad \text{for} \quad \delta\overline{\boldsymbol{\varepsilon}} = [0\,0\,0], \quad \delta\overline{\boldsymbol{\eta}} = [1\,0\,0\,0\,0\,0],\\
&\delta\overline{\boldsymbol{\sigma}}^2: \quad \text{for} \quad \delta\overline{\boldsymbol{\varepsilon}} = [0\,0\,0], \quad \delta\overline{\boldsymbol{\eta}} = [0\,1\,0\,0\,0\,0],\\
&\delta\overline{\boldsymbol{\sigma}}^3: \quad \text{for} \quad \delta\overline{\boldsymbol{\varepsilon}} = [0\,0\,0], \quad \delta\overline{\boldsymbol{\eta}} = [0\,0\,1\,0\,0\,0],\\
&\delta\overline{\boldsymbol{\sigma}}^4: \quad \text{for} \quad \delta\overline{\boldsymbol{\varepsilon}} = [0\,0\,0], \quad \delta\overline{\boldsymbol{\eta}} = [0\,0\,0\,1\,0\,0],\\
&\delta\overline{\boldsymbol{\sigma}}^5: \quad \text{for} \quad \delta\overline{\boldsymbol{\varepsilon}} = [0\,0\,0], \quad \delta\overline{\boldsymbol{\eta}} = [0\,0\,0\,0\,1\,0],\\
&\delta\overline{\boldsymbol{\sigma}}^3: \quad \text{for} \quad \delta\overline{\boldsymbol{\varepsilon}} = [0\,0\,0], \quad \delta\overline{\boldsymbol{\eta}} = [0\,0\,0\,0\,0\,1].
\end{aligned} \tag{33}$$

Material tangent stiffness matrix $\overline{\mathbf{C}}^3$ is computed as

$$\overline{\mathbf{C}}^3 = [\,\delta\overline{\boldsymbol{\tau}}^1\,,\,\delta\overline{\boldsymbol{\tau}}^2\,,\,\delta\overline{\boldsymbol{\tau}}^3\,], \tag{34}$$

where columns $\delta\overline{\boldsymbol{\tau}}^i$, $i = 1,2,3$, are computed for given increments of the strain vector,

$$\begin{aligned}
&\delta\overline{\boldsymbol{\tau}}^1: \quad \text{for} \quad \delta\overline{\boldsymbol{\varepsilon}} = [1\,0\,0], \quad \delta\overline{\boldsymbol{\eta}} = [0\,0\,0\,0\,0\,0],\\
&\delta\overline{\boldsymbol{\tau}}^2: \quad \text{for} \quad \delta\overline{\boldsymbol{\varepsilon}} = [0\,1\,0], \quad \delta\overline{\boldsymbol{\eta}} = [0\,0\,0\,0\,0\,0],\\
&\delta\overline{\boldsymbol{\tau}}^3: \quad \text{for} \quad \delta\overline{\boldsymbol{\varepsilon}} = [0\,0\,1], \quad \delta\overline{\boldsymbol{\eta}} = [0\,0\,0\,0\,0\,0].
\end{aligned} \tag{35}$$

Material tangent stiffness matrix $\overline{\mathbf{C}}^4$ is computed as

$$\overline{\mathbf{C}}^4 = [\,\delta\overline{\boldsymbol{\tau}}^1\,,\,\delta\overline{\boldsymbol{\tau}}^2\,,\,\delta\overline{\boldsymbol{\tau}}^3\,,\,\delta\overline{\boldsymbol{\tau}}^4\,,\,\delta\overline{\boldsymbol{\tau}}^5\,,\,\delta\overline{\boldsymbol{\tau}}^6\,], \tag{36}$$

where columns $\delta\overline{\boldsymbol{\tau}}^i, i = 1,2,3$ are computed for given increments of the higher order strain vector,

$$\begin{aligned}
&\delta\overline{\boldsymbol{\tau}}^1: \quad \text{for} \quad \delta\overline{\boldsymbol{\varepsilon}} = [0\,0\,0], \quad \delta\overline{\boldsymbol{\eta}} = [1\,0\,0\,0\,0\,0],\\
&\delta\overline{\boldsymbol{\tau}}^2: \quad \text{for} \quad \delta\overline{\boldsymbol{\varepsilon}} = [0\,0\,0], \quad \delta\overline{\boldsymbol{\eta}} = [0\,1\,0\,0\,0\,0],\\
&\delta\overline{\boldsymbol{\tau}}^3: \quad \text{for} \quad \delta\overline{\boldsymbol{\varepsilon}} = [0\,0\,0], \quad \delta\overline{\boldsymbol{\eta}} = [0\,0\,1\,0\,0\,0],\\
&\delta\overline{\boldsymbol{\tau}}^4: \quad \text{for} \quad \delta\overline{\boldsymbol{\varepsilon}} = [0\,0\,0], \quad \delta\overline{\boldsymbol{\eta}} = [0\,0\,0\,1\,0\,0],\\
&\delta\overline{\boldsymbol{\tau}}^5: \quad \text{for} \quad \delta\overline{\boldsymbol{\varepsilon}} = [0\,0\,0], \quad \delta\overline{\boldsymbol{\eta}} = [0\,0\,0\,0\,1\,0],\\
&\delta\overline{\boldsymbol{\tau}}^3: \quad \text{for} \quad \delta\overline{\boldsymbol{\varepsilon}} = [0\,0\,0], \quad \delta\overline{\boldsymbol{\eta}} = [0\,0\,0\,0\,0\,1].
\end{aligned} \tag{37}$$

We can see that only the right-hand side of the linear equations is different for each case, so after the LU decomposition of the left-hand side of the linear equations the computation of tangent stiffness matrices can be made efficiently.

4. Numerical example

In this section a thin layer shear problem is investigated. Microstructurally a porous material is analyzed numerically. For the numerical solution of the macroscale problem, the finite element mesh indicated in Fig. 3 is used. The mesh consists of plane strain quadrilateral elements for the second-order continuum in [10]. Since for this problem all quantities are independent of x, one single row of elements is needed. The heights of shear layer are $H = 10.0\,\text{mm}$ and $H = 1.0\,\text{mm}$. Vertical displacements are equal zero between left-hand and right-sides.

A material with randomly distributed voids is analysed. For modelling at the microscale, two RVEs in Fig. 4 are shown. It can be noted that RVEs with different statistical representation are analysed. The characteristic size of RVEs is $L = 0.6\,\text{mm}$ and the volume fraction is $V_\text{f} \approx 0.12$. The voids are modelled by Level Set Method in XFEM. The finite element mesh at microscale contains constant strain triangular elements and has a characteristic size $h^e = 0.008\,\text{mm}$. The matrix material is assumed to be elastic with Hooke's constitutive equation and materials parameters: Young's modulus $E = 210\,\text{GPa}$ and Poison's ratio $\nu = 0.3$. Because the investigated material has a random distribution of voids, for each type of RVEs (with small and large voids) and for each height of shear layer, 100 numerical simulations are analysed.

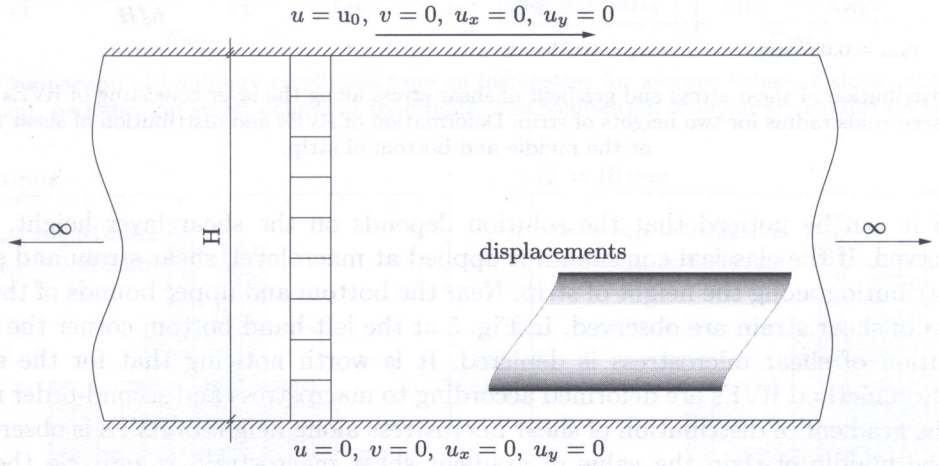

Fig. 3. Geometry, boundary conditions, and the finite element mesh for boundary shear layer problem

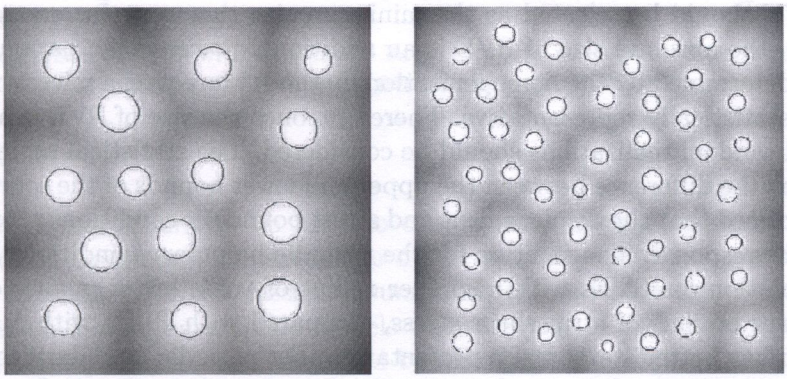

Fig. 4. RVEs consisting of voids with radius $r_\text{ave} = 0.032\,\text{mm}$ and $r_\text{ave} = 0.016\,\text{mm}$

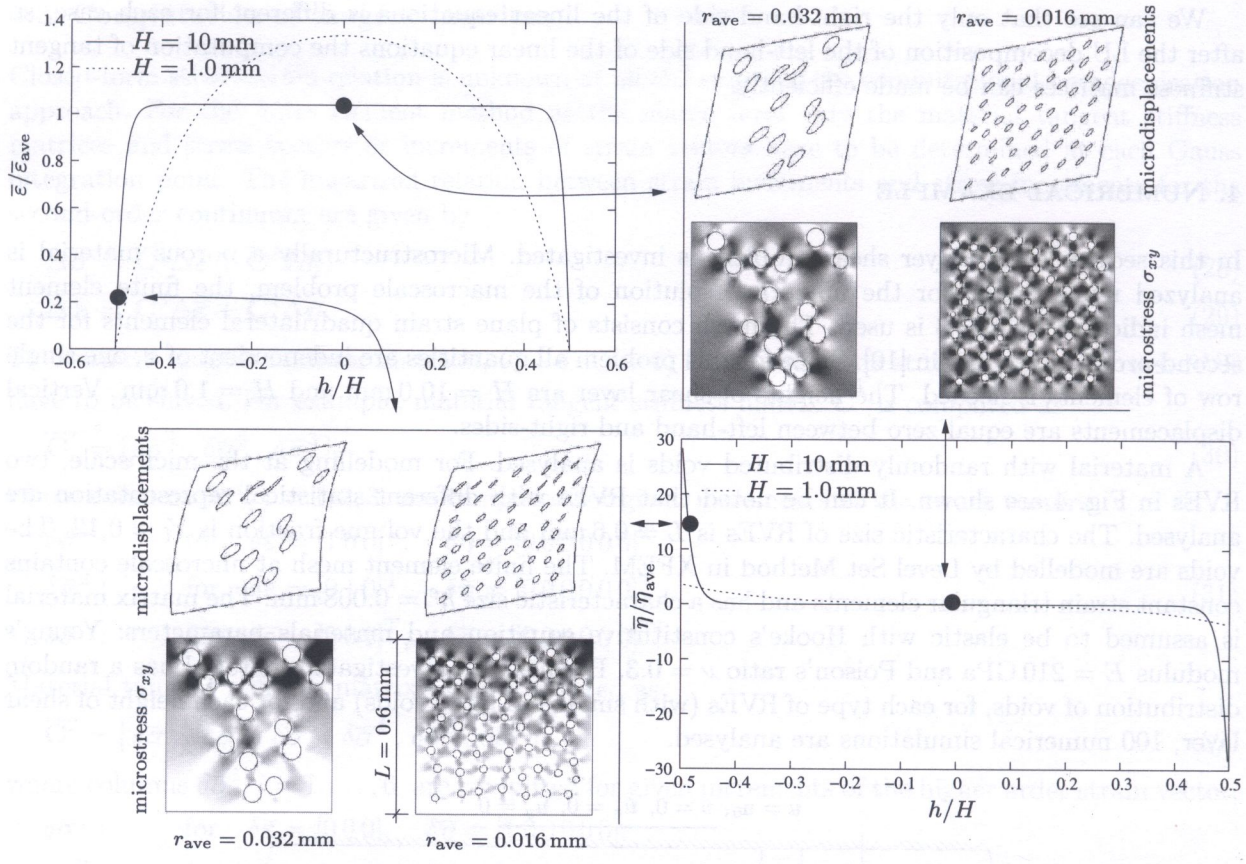

Fig. 5. Distribution of shear stress and gradient of shear stress along the layer consisting of RVEs with small void and large voids radius for two heights of strip. Deformation of RVEs and distribution of shear microstress at the middle and bottom of strip.

In Fig. 5 it can be noticed that the solution depends on the shear layer height, i.e. the size effect is observed. If the classical continuum is applied at macrolevel, shear strain and stress have a constant distribution along the height of strip. Near the bottom and upper bounds of the shear layer the gradients of shear strain are observed. In Fig. 5 at the left-hand bottom corner the deformation and distribution of shear microstress is depicted. It is worth noticing that for the second-order homogenisation method RVEs are deformed according to macrostress and second-order macrostrain. Moreover, the gradient of distribution of shear microstress along height of RVEs is observed. Despite of this, in the middle of strip the value of gradient shear macrostrain is zero. So the pure shear deformation of RVEs in Fig. 5 at the upper right corner can be noticed. Distributions of shear microstress are uniform in RVEs.

The size of RVE should be selected as the minimum size that contains enough microstructural features. However, the absolute size of RVE is an additional macroscopic parameters of the model which can not be determined by the homogenisation method. Moreover, a microstructural cell size of RVE may not be statistically representative. Therefore, once the size of RVE is assumed, a number of microstructural random realizations should be considered. The statistical representation of RVEs can be measured by the difference between the upper and lower bounds of the solution. A well known property can be noticed that the displacement and stress boundary conditions provide the upper and lower bounds of the response. The solution for the periodic boundary conditions lies between them, see Fig. 6. The solution for RVEs with a smaller radius of voids has a smaller difference between the upper and lower bounds of strip shear stress, compared with RVEs with a smaller number of voids, the solution has better statistical representation. For periodic boundary conditions a smaller variance of solution is observed for random distribution of voids in Fig. 7. It can also be noticed that the solution on average compared to the same value for different numbers of voids in RVEs.

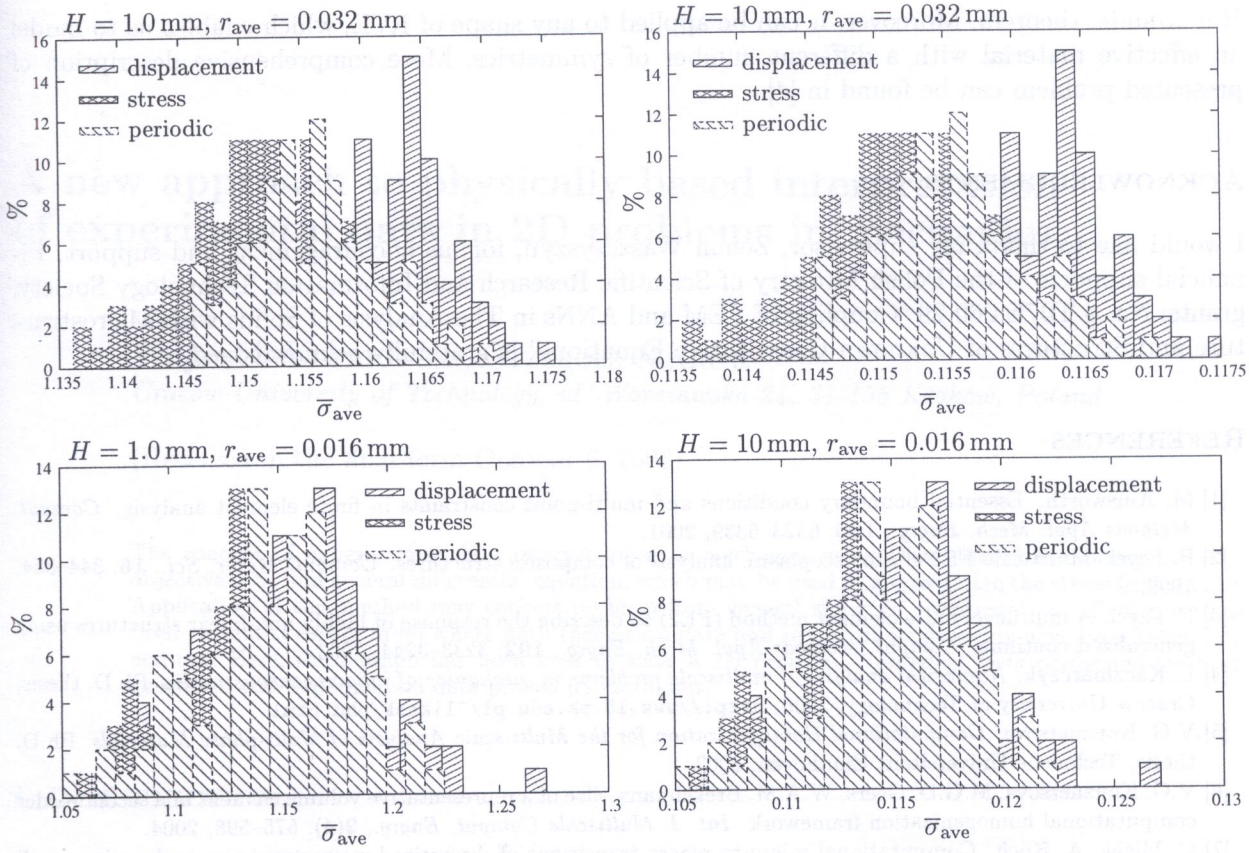

Fig. 6. Comparison of boundary conditions type on histograms for average values of shear macrostress for displacement, periodic and stress boundary conditions. The comparison of boundary conditions type

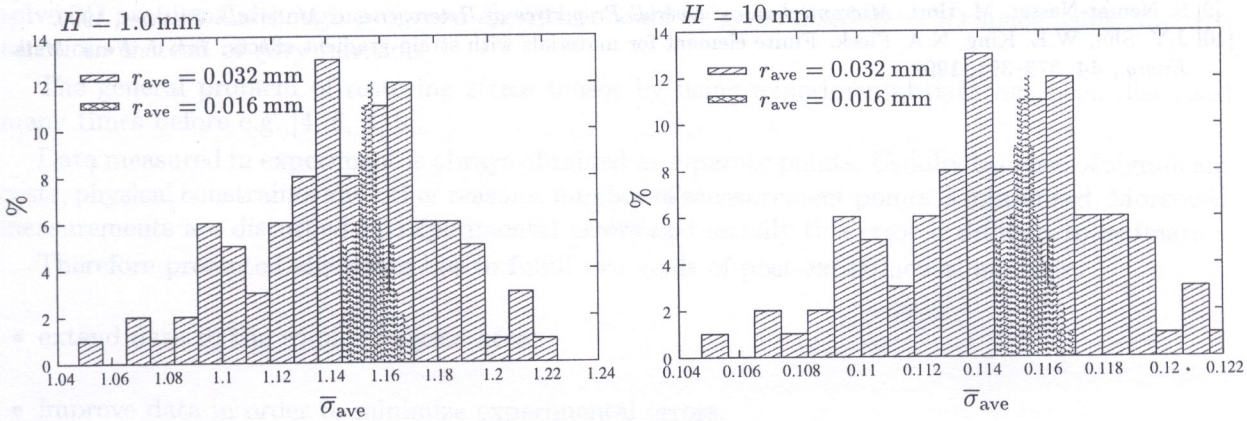

Fig. 7. The comparison of RVEs with smaller and larger radius of voids on histograms for averaged values of shear macrostress for periodic boundary conditions

5. Conclusions

Computational homogenisation can be used to couple two different continua at macroscale, i.e. classical and gradient continua. The advantage of the second-order homogenisation framework is that it allows one to escape from the classical assumption of scale separation. Taking into account the size effects enables us to apply multiscale models when the size of RVE does not vanish. Moreover, when localisation takes place, the results should be meaningful.

In the paper a method of enforcing boundary condition for micro-to-macro transitions has been proposed. The method enables us to enforce any type of boundary conditions consistent with the

Hill–Mandel theorem. Moreover, it can be applied to any shape of RVE, which enables us to model an effective material with a different number of symmetries. More comprehensive description of presented problem can be found in [4].

Acknowledgments

I would like to thank my supervisor, Zenon Waszczyszyn, for his encouragement and support. Financial supports of the Polish Ministry of Scientific Research and Information Technology Society, grants: No. 4 T07E 060 29 "Coupling of FEM and ANNs in The Analysis of Solids with Microstructure and Structures of Unknown Constitutive Equations" is gratefully acknowledged.

References

[1] M. Ainsworth. Essential boundary conditions and multi-point constraints in finite element analysis. *Comput. Methods Appl. Mech. Engrg.*, **190**: 6323–6339, 2001.

[2] F. Feyel. Multiscale FE2 elastoviscoplastic analysis of composite structures. *Comput. Mater. Sci.*, **16**: 344–354, 1999.

[3] F. Feyel. A multilevel finite element method (FE2) to describe the response of highly non-linear structures using generalized continua. *Comput. Methods Appl. Mech. Engrg.*, **192**: 3233–3244, 2003.

[4] L. Kaczmarczyk. *Numerical analysis of multiscale problems in mechanics of inhomogeneous media.* Ph.D. thesis, Cracow University of Technology, 2006, `http://www.l5.pk.edu.pl/~likask/phd.html`

[5] V.G. Kouznetsova. *Computational Homogenization for the Multi-scale Analysis of Multi-phase Materials.* Ph.D. thesis, Technishe Universiteit, Eindhoven, 2002.

[6] V.G. Kouznetsova, M.G.D. Geers, W.A.M. Brekelmans. Size of a representative volume element in a second-order computational homogenization framework. *Int. J. Multiscale Comput. Engrg.*, **2**(4): 575–598, 2004.

[7] C. Miehe, A. Koch. Computational micro-to-macro transitions of discretized microstructures undergoing small strains. *Arch. Appl. Mech.*, **72**: 300–317, 2002.

[8] R.D. Mindlin. Second gradient of strain and surface-tension in linear elasticity. *Int. J. Solids Struct.*, **1**: 417–438, 1965.

[9] S. Nemat-Nasser, M. Hori. *Micromechanics: Overall Properties of Heterogeneous Materials.* Elsevier, 1999.

[10] J.Y. Shu, W.E. King, N.A. Fleck. Finite element for materials with strain gradient effects. *Int. J. Num. Meth. Engrg.*, **44**: 373–391, 1999.